Society For Biomaterials

# Titanium dioxide nanoparticle-induced dysfunction of cardiac hemodynamics is involved in cardiac inflammation in mice

**Fashui Hong,[1,2,3] Nan Wu,[1,2,3] Xiangyu Zhao,[1,2,3] Yusheng Tian,[1,2,3] Yingjun Zhou,[1,2,3] Ting Chen,[1,2,3] Yanyu Zhai,[1,2,3] Li Ji[1,2,3]**

[1]Jiangsu Collaborative Innovation Center of Regional Modern Agriculture & Environmental Protection, Huaiyin Normal University, Huaian 223300, China
[2]Jiangsu Key Laboratory for Eco-Agricultural Biotechnology around Hongze Lake, Huaiyin Normal University, Huaian 223300, China
[3]School of Life Sciences, Huaiyin Normal University, Huaian 223300, China

Received 5 May 2016; revised 24 June 2016; accepted 7 July 2016
Published online 00 Month 2016 in Wiley Online Library (wileyonlinelibrary.com). DOI: 10.1002/jbm.a.35831

**Abstract:** In the past two decades, titanium dioxide nanoparticles ($TiO_2$ NPs) have been extensively used in medicine, food industry and other daily life, while their possible interactions with the their influence and human body on human health remain not well understood. Thus, the study was designed to examine whether long-term exposure to $TiO_2$ NPs cause myocardial dysfunction which is involved in cardiac lesions and alter expression of genes and proteins involving inflammatory response in the mouse heart. The findings showed that intragastric feeding for nine consecutive months with $TiO_2$ NPs resulted in titanium accumulation, infiltration of inflammatory cells and apoptosis of heart, reductions in net increases of body weight, cardiac indices of function (LV systolic pressure, maximal rate of pressure increase over time, maximal rate of pressure decrease over time and coronary flow), and increases in heart indices, cardiac indices of function (LV end-diastolic pressure and heart rate) in mice. $TiO_2$ NPs also decreased ATP production in the hearts. Furthermore, $TiO_2$ NPs increased expression of nuclear factor-κB, interleukin-lβ and tumour necrosis factor-α, and reduced expression of anti-inflammatory cytokines including suppressor of cytokine signaling (SOCS) 1 and SOCS3 in the cardiac tissue. These results suggest that $TiO_2$ NPs may modulate the cardiac function and expression of inflammatory cytokines. © 2016 Wiley Periodicals, Inc. J Biomed Mater Res Part A: 00B:000–000, 2016.

**Key Words:** titanium dioxide nanoparticles, mice, cardiac hemodynamics, inflammation, apoptosis

**How to cite this article**: Hong F, Wu N, Zhao X, Tian Y, Zhou Y, Chen T, Zhai Y, Ji L. 2016. Titanium dioxide nanoparticle-induced dysfunction of cardiac hemodynamics is involved in cardiac inflammation in mice. J Biomed Mater Res Part A 2015:00A:000–000.

## INTRODUCTION

Titanium dioxide nanoparticles (TiO2 NPs) are widely used in everyday life products, for example, household items, cosmetics, food packaging systems, food additives, toothpaste, and paints,[1,2] and in medicine, including pharmaceuticals, diagnosis, therapeutics, and tissue engineering,[3–5] and also used in removal of environmental pollutions.[6–10] Due to common use of TiO2 NPs in various areas, it may pose consumer and occupational risks, thus about their toxicity and their potential harmful influence on human health and environment have been highly concerned. Numerous experimental evidences proved that once present in the circulation, TiO2 NPs could reach and accumulate in animal organs and cause their lesions including liver, kidney, lung, spleen, brain, ovary, and testis.[11–21] Importantly, it has been suggested that NPs including $TiO_2$ NPs can be translocated to heart, cause myocardial dysfunction, oxidative stress, cardiac inflammation and atherosclerosis in mice,[22–26] induce plaque progression in aorta of mice,[27] endothelial inflammatory response in primary vascular endothelial cells,[28] and cardiac infarction in rats.[29] As known, cardiac inflammation adversely affects cardiopulmonary hemodynamics in animals and human.[30–33] Hemodynamics is a hydrodynamic problem for studying the flow of blood in the cardiovascular system, its basic research object is the relationship between flow resistance and pressure, and studies the effect of drugs on the cardiac function of the organism, pharmacological effects, and mechanisms of cardiovascular drugs. However, effects of $TiO_2$ NPs on myocardial functions have not been addressed extensively, with their molecular mechanisms on intracellular targets being largely unknown and unproved. Especially, whether $TiO_2$ NPs influence cardiac hemodynamics due to cardiac lesions remains unclear.

Fashui Hong, Nan Wu, and Xiangyu Zhao contributed equally to this work.
**Correspondence to:** F. Hong; e-mail: hfshui666@126.com

A noticeable aging of the population and a higher risk of developing of cardiovascular disorders among the elderly people raises the question of the role of NPs, and NPs in particular, in these processes. It was shown that accumulation of NPs in the lung and heart may induce inflammation, vasomotor dysfunction and cardiovascular lesions followed by adverse long term effects.[34–38] We hypothesized that cardiac inflammation by exposure to TiO2 NPs may impair myocardial functions. Hence, this work is focused on the effects of TiO2 NPs on cardiac indices including left ventricular pressure (LVDP), heart rate (HR), LV end-diastolic pressure (LVEDP), LV systolic pressure (LVSP), maximal rate of pressure increase over time ($dp/dt_{max}$), maximal rate of pressure decrease over time ($dp/dt_{min}$) and coronary flow (CF) and NF-κB, proinflammatory cytokines, and anti-inflammatory cytokines in the mouse heart. Therefore, taking into account possible harmful action of TiO2 NPs, the aim of this study was to explore effects of TiO2 NPs on cardiac hemodynamics, inflammatory response, and expression of inflammatory response-related molecules in the mouse heart.

## MATERIALS AND METHODS

### Chemicals

The preparation and characterization of nano $TiO_2$ were performed as Yang's previously study,[39] and our previously described;[40] the characterization was as follows: anatase for phase, $5-6$ nm for particle size, mainly 295 nm for hydrodynamic diameter, 174.8 $m^2/g$ for surface area, and 9.28 mV for zeta potential, respectively.[39,40]

### Animals and treatment

One hundred and sixty ICR (Imprinting Control Region) male mice, aged 5 weeks with a mean body mass of $22 \pm 2$ g, were purchased from the Animal Center of Soochow University (Jiangsu, China). All procedures performed on the animals were approved by the Institutional Animal Care and Use Committee of Huaiyin Normal University, and thus within the guidelines for human care of laboratory animals for scientific purposes. Both water and food were provided with casual.

An hydroxypropylmethylcellulose (HPMC) K4M (Sigma-Aldrich, St. Louis, MO, USA) concentration of 0.5% was used as a suspending agent. $TiO_2$ NPs powder was dispersed onto the surface of 0.5% w/v HPMC solution, and then the suspending solutions containing $TiO_2$ NPs were treated ultrasonically for 30 min and mechanically vibrated for 5 min. During the experiment, the mice were randomly divided into four groups ($n = 40$ each), including a control group (treated with 0.5% w/v HPMC) and three experimental groups (1.25, 2.5, or 5 mg/kg BW of $TiO_2$ NPs). For dose selection, we accorded to references, for example, dietary exposure to $TiO_2$ in Western populations is $1-3$ mg/kg body weight day of $TiO_2$ on average for children under the age of 10 years.[41] Assuming that 36% of food-grade $TiO_2$ is smaller than 100 nm in at least one dimension, this exposure limit decreases to approximately 0.1 mg/person day of nanoscale $TiO_2$.[42] All mice were weighed, the $TiO_2$ NPs suspensions of different doses were administered to mice by intragastric feeding every other day for 9 months.

### Assay of cardiac hemodynamics

Mice were anesthetized by intraperitoneal injection of pentobarbital 50 mg/kg (0.1 mL/100 g bodyweight) and heparinized i.p. (0.1 mL 500 IU/100 g bodyweight). Anesthesia was examined by the pedal–withdrawal reflex. The heart was rapidly excised and immediately placed in cold (4°C) Krebs–Henseleit buffer (KHBB) (in mmol/L, glucose 17, NaCl 120, $NaHCO_3$ 25, $CaCl_2$ 2.5, KCl 5.9, $MgSO_4$ 1.2, and EDTA 0.5) to temporarily stop its beating and preserve it from ischemic injury prior to perfusion. The heart was mounted on a steel cannula placed in the aorta and perfused retrogradely in a Langendorff system with the use of thermostated (37°C) reservoirs (Nanjing Medease Technology, Nanjing, China), perfusion lines and heart chamber. Pressure regulated flow was performed at 100 cm $H_2O$ (73 mmHg) with KHBB, and volume regulated flow (10.5 mL/min) was performed using a peristaltic pump (Nanjing Medease Technology, Nanjing, China). To record left ventricular pressure (LVDP) and secondarily derived contractility indices, a water-filled latex balloon was placed in the left ventricle and linked to a pressure transducer (Nanjing Medease Technology, Nanjing, China). The raw data signal were amplified, and analyzed using Medlab-U/4CS biological signal acquisition and processing systema (Nanjing Medease Technology, Nanjing, China) on a personal computer. The program performs calculation of HR, LVEDP, LVSP, $dp/dt_{max}$, $dp/dt_{min}$ and CF. The left ventricular pressure parameters were calculated every 5 s and the raw data transferred to an Excel (Microsoft, Seattle) file for further calculations. All experiments and analysis were carried out between 7 am and 7 pm.

### Assay of heart indices

After weighing the body and hearts, the heart indices were calculated as the ratio of heart (wet weight, mg) to body weight (g).

### Titanium content analysis

Approximately 0.2 g of the heart was weighed, digested, and analyzed for titanium content. Inductively coupled plasma-mass spectrometry ([ICP-MS] Thermo Elemental X7; Thermo Electron, USA) was used to analyze the titanium concentration in the samples.

### Histopathological evaluation

After fixation in 10% neutral formalin, and embedded in paraffin, hearts ($n = 5$ in each group) were sliced at a thickness of 5 μm, and placed on separate glass slides. After hematoxylin and eosin staining, the heart simples were routinely evaluated by a histopathologist unaware of the treatments for light microscopy (U-III Multi-point Sensor System; Nikon, Tokyo, Japan).

**TABLE I. Real-Time PCR Primer Pairs**

| Gene Name | Description | Primer Sequence | Primer Size (bp) |
|---|---|---|---|
| Refer-GAPDH | mGAPDH-F | 5′-TGTGTCCGTCGTGGATCTGA-3′ | |
| | mGAPDH-R | 5′-TTGCTGTTGAAGTCGCAGGAG-3′ | 150 |
| NF-κB | mNF-κB-F | 5′-GTGGAGGCATGTTCGGTAGTG-3′ | |
| | mNF-κBR | 5′-TCTTGGCACAATCTTTAGGGC-3′ | 195 |
| IL-1β | mIL-1β-F | 5′-GCTTCAGGCAGGCAGTATCA-3′ | |
| | mIL-1β-R | 5′-TGCAGTTGTCTAATGGGAACG-3′ | 196 |
| TNF-α | mTNF-α-F | 5′-CCCTCCAGAAAAGACACCATG-3′ | |
| | mTNF-α-R | 5′-CACCCCGAAGTTCAGTAGACAG-3′ | 183 |
| SOCS1 | mSOCS1-F | 5′-CCGCTCCCACTCCGATTAC-3′ | |
| | mSOCS1-R | 5′-CGAAGAAGCAGTTCCGTTGG-3′ | 167 |
| SOCS3 | mSOCS3-F | 5′-CCAGTCGGGGACCAAGAAC-3′ | |
| | mSOCS3-R | 5′-TGGGTGGCAAAGAAAAGGAG-3′ | 164 |

PCR primers used in the gene expression analysis.

### Observation of cardiac ultrastructure

Hearts ($n = 5$ in each group) were fixed in a fresh solution of 0.1*M* sodium cacodylate buffer containing 2.5% glutaraldehyde and 2% formaldehyde followed by a 2 h fixation period at 4°C with 1% osmium tetroxide in 50 m*M* sodium cacodylate (pH 7.2–7.4). Staining was performed overnight with 0.5% aqueous uranyl acetate. The hearts were dehydrated in a graded series of ethanol (75, 85, 95, and 100%), and embedded in Epon 812. Ultrathin sections were obtained, contrasted with uranyl acetate and lead citrate, and observed with a HITACHI H600 Transmission Electron Microscope (HITACHI, Japan).

### Assay of ATP

ATP was measured using bioluminescence based on the luciferineluciferase reaction[43] and was measured with commercially-available kits (Genmed Scientifics, USA). The samples were pipetted into 96-well luminometer plates. The nucleotides were released from the cell suspensions by the addition of an equal volume of cell nucleotide-releasing reagent. This releasing reagent also contained the luciferineluciferase, nucleotide-monitoring reagent. The ATP levels were measured using a luminometer (Lucy 1, Anthos, Luminoskan, Labsystems, USA) and expressed as the number of relative light units (RLU). Under these optimal conditions and at concentrations of ATP less than 10*M*, the RLU were directly proportional to the amount of ATP present. The ATP signal was allowed to decay for 10 min to a steady state. After 10 min, a reading was taken to determine the baseline ADP RLU (ADP 0). The ADP in the wells was converted to ATP by the addition of 5 mL of ADP converting reagent. After 1 min incubation to allow for conversion of ADP to ATP, a third reading was taken (ADP). The ratio of ADP: ATP for each well was calculated from these three readings as follows: ADP/ATP ratio¼(ADP RLU − ADP 0 RLU)/ATP RLU.

### Assay of cytokine expression

Total RNA was extracted from individual hearts ($n = 5$ in each group) with Tripure Isolation Reagent (Roche, USA) according to the manufacturer's protocol. According to MIQE guidelines, probes and cycling conditions were optimized for PCR. cDNA was reverse transcribed from total RNA samples using the TaqMan RT reagents (Applied Biosystems, USA) and used for real-time PCR by employing primers designed using Primer Express Software according to the software guidelines. Primer sets were used for real-time PCR assays and are exhibited in Table I. The probes for NF-κB, IL-lβ, TNF-α, SOCS1, and SOCS3 in the hearts were designed by the manufacturer and purchased from Shinegene Company (Shanghai, China). As endogenous references for these PCR quantification studies, glyceraldehyde-3-phosphate dehydrogenase(GAPDH) gene expression was measured. The data were assayed by the Rotor Gene 6000 v.1.7 software. Relative gene expression was determined using the Relative Expression Software Tool 2008,[44] and NormFinder software.[45]

### Western blot

Cardiac tissues were homogenized in ice-cold RIPA lysis buffer (50 m*M* Tris–HCl (pH 7.4), 150 m*M* NaCl, 1% NP-40, 0.1% SDS), and protease inhibitor was added with the dose of 1% RIPA lysis buffer. Total protein(30–50 μg) was subjected to 8 or 12% SDS-PAGE, transferred to nitrocellulose membranes, and incubated with primary antibodies: anti-NF-κB(1:500), anti-IL-lβ(1:500), anti-TNF-α(1:500), anti-IFN-α (1:500), anti-SOCS1(1:500) and anti-SOCS3(1:500), and anti-β-actin (1:2000). After washing with TBST three times, the membrane was incubated with horseradish peroxidase (HRP)-conjugated secondary antibodies (1:10000) (Longshengtianshi Biotechnology Company, Suzhou, China) at room temperature for 2 h, followed by detection using enhanced chemiluminescence (ECL, Millipore, Bedford, MA, USA). Immunoreactive bands were visualized using X-ray films. For quantitative analysis, bands were evaluated with ImageJ software, normalized for β-actin density.

### Statistical analysis

Data were represented as mean ± standard deviation (SD). Statistical analyses were performed by a SPSS 19.0 software (Chicago, IL, USA) and statistical comparisons were analyzed using one-way ANOVA followed by Tukey's HSD *post hoc*

**TABLE II. Effect of Chronic $TiO_2$ NPs Exposure on Body Weight, Cardiac Indices of Mice and Titanium Content in the Heart for Nine Consecutive Months**

| | $TiO_2$ NPs (mg/kg BW) | | | |
|---|---|---|---|---|
| Index | Control | 1.25 | 2.5 | 5 |
| Net increases of body weight (g) | 25.56 ± 3.16a | 23.61 ± 2.09a | 20.12 ± 2.46b | 17.45 ± 2.17c |
| Heart indices (mg/g) | 5.15 ± 0.45a | 5.33 ± 0.35a | 6.48 ± 0.41b | 6.62 ± 0.62b |
| *Ti content (ng/g tissue)* | 8.55 ± 0.83a | 201.37 ± 36.19b | 329.61 ± 27.17c | 508.46 ± 31.92d |

Different letters in the same parameter indicate significant differences between groups ($p < 0.05$). Values represent mean ± SD ($N = 5$).

test. Differences were considered statistically significant when the $p$ values was less than 0.05.

## RESULTS

### Body weight, cardiac indices, and titanium content

Effects of $TiO_2$ NPs exposure on body weight, cardiac indices, and titanium accumulation of mice are exhibited in Table II. It can be observed that $TiO_2$ NPs exposure remarkably reduced net increases of body weight, with reductions of 7.63, 21.28, and 31.73%, respectively; whereas $TiO_2$ NPs exposure increased heart indices, with increases of 3.5, 25.83, and 28.54%, respectively. With increasing $TiO_2$ NPs dose, titanium contents in the heart were greatly increased (Table II), suggesting that the cardiac toxicity may be related to $TiO_2$ NPs accumulation in the heart.

### Isolated heart parameters

Table III summarizes effects of $TiO_2$ NPs exposure on cardiac hemodynamics of mice after 30 min of equilibration in isolated mouse hearts perfused at constant pressure. It can be seen that with increasing $TiO_2$ NPs dose, LVEDP, and HR were significantly increased by 81.39, 98.11, and 150.0%; and 8.38; 15.58, and 27.26%, respectively; whereas LVSP, $dp/dt_{max}$, $dp/dt_{min}$, and CF were obviously decreased by 20.32, 29.96, and 44.56%; 10.16, 20.8, and 25.34%; 4.0, 11.2, and 26.96%; 24.14, 30.85, and 39.29%, respectively. It indicates that $TiO_2$ NPs caused the cardiac damage and cardiac dysfunction of mice, which is confirmed by the further the morphological examination of heart and assay of biochemical parameters in the heart.

### Histopathological observation

Figure 1 shows histopathological changes of the heart. Hearts from mice exposed to $TiO_2$ NPs displayed local infiltration of inflammatory cells, sparse myocardial fibers, disorder of muscle cell array, partial myocardial necrosis, congestion of partial blood vessel, and partial bleeding (Fig. 1), but unexposed heart samples (control) did not present the lesions (Fig. 1).

### Observation of ultrastructure

Changes to the myocardial cell ultrastructure are presented in Figure 2. As shown, cardiac cell of the control group exhibited neat muscle fibers and stripes, normal mitochondria, and nuclei (Fig. 2); however, ultrastructure of myocardial cell treated with $TiO_2$ indicated a typical apoptosis, including significant chromatin aggregation, mitochondrial swelling, disorder or disappearance of mitochondrial crest, dilation and swelling of endoplasmic reticulum, and $TiO_2$ NPs deposition (Fig. 2). In addition, disorders of muscle fibers caused by $TiO_2$ NPs were observed (Fig. 2).

### ATP assay

To further suggested that $TiO_2$ NPs disrupted the mitochondrial electron transport chain (ETC) and decreased the production of mitochondrial energy in the heart, we investigated mitochondrial energy ATP and ADP derived primarily from the hydrolysis of ATP. Figure 3 shows that $TiO_2$ NPs decreased the production of ATP, and the ADP/ATP ratio was increased by 3.21-, 4.55-, and 9.64-fold, as compared with the control.

### Expression of inflammatory cytokines

To confirm whether $TiO_2$ NPs exposure resulted in alterations of NF-κB, inflammatory cytokine gene and protein expression, including TNF-α, IL-1β, SOCS1, and SOCS3, in the $TiO_2$ NP-induced heart injury, real-time quantitative RT-PCR and Western blot were used to detect levels in these cytokine expression in the $TiO_2$ NP-exposed heart and

**TABLE III. Effects of Chronic $TiO_2$ NPs Exposure on Cardiac Hemodynamics of Mice for Nine Consecutive Months**

| | $TiO_2$ NPs (mg/kg BW) | | | |
|---|---|---|---|---|
| Index | Control | 1.25 | 2.5 | 5 |
| LVSP (mmHg) | 19.59 ± 2.15a | 15.61 ± 1.41b | 13.72 ± 1.15b | 10.86 ± 1.07c |
| LVEDP (mmHg) | 10.05 ± 1.98a | 18.23 ± 2.05b | 19.91 ± 1.85c | 25.13 ± 2.78d |
| $dp/dt_{max}$ (mmHg/s) | 5875 ± 298a | 5278 ± 308b | 4653 ± 891c | 4386 ± 1094c |
| $dp/dt_{min}$ (mmHg/s) | 5096 ± 139a | 4892 ± 183a | 4525 ± 161b | 3722 ± 115.73c |
| HR (bpm) | 383.59 ± 13.08a | 415.72 ± 12.23b | 443.33 ± 10.08c | 488.15 ± 15.52d |
| *CF (ml/min)* | 13.13 ± 2.97a | 9.96 ± 2.32b | 9.08 ± 1.43b | 7.97 ± 1.51c |

Different letters in the same parameter indicate significant differences between groups ($p < 0.05$). Values represent mean ± SD ($N = 5$).

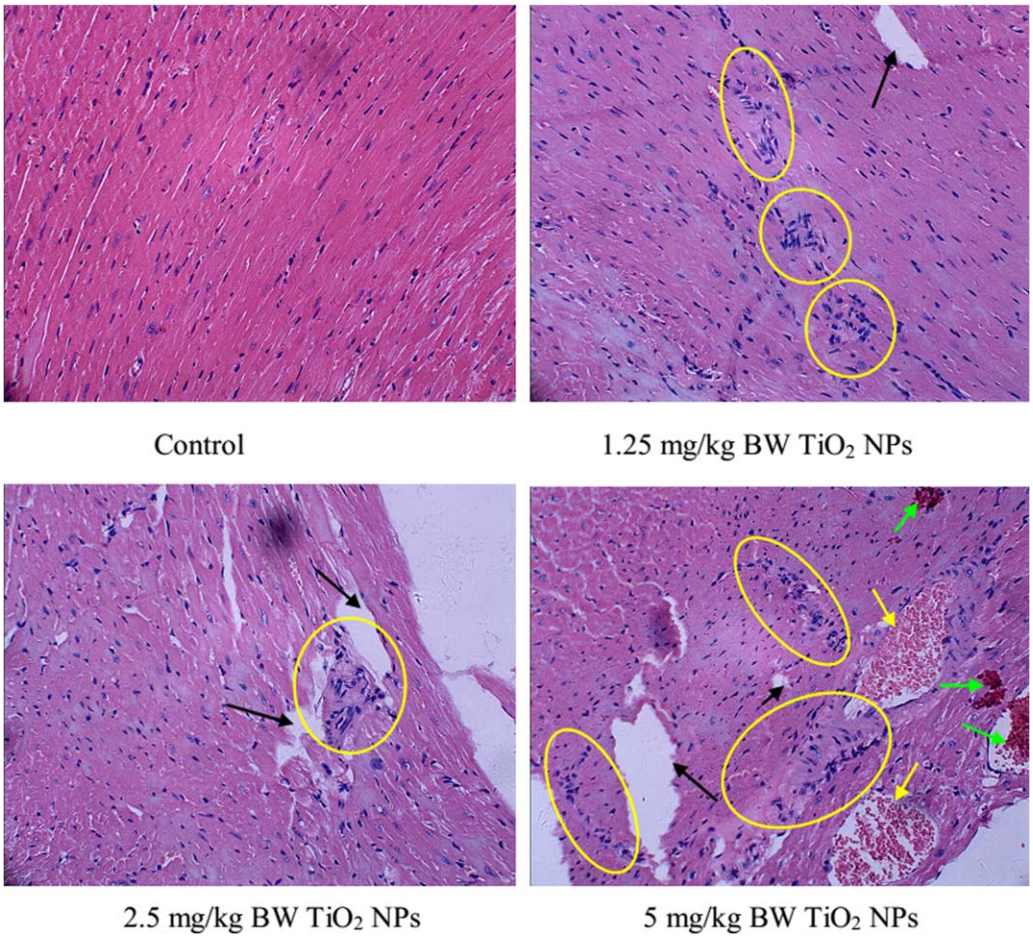


**FIGURE 1**. Histopathological observations of hearts in mice following exposure to $TiO_2$ NPs for nine consecutive months (200×). Yellow circle indicated infiltration of inflammatory cells; black arrow indicated tissue necrosis; green arrow indicated bleeding; yellow arrow indicated congestion of blood vessel.

presented in Table IV and Figure 4. It indicated that with increasing $TiO_2$NPs doses, levels of NF-κB, IL-lβ, and TNF-α gene or protein expression were remarkably elevated from 22.4 to 1127.66%, 34.05 to 109.09%, and 19.67 to 104.0%, respectively; but levels of SOCS1 and SOCS3 gene or protein expression were significantly decreased from 15.07 to 53.42%, and 22.76 to 66.44% in the cardiac tissue, respectively (Table IV; Fig. 4).

## DISCUSSION

Data on the toxic effect of NPs on the cardiovascular system function are relatively limited in numerous previous studies, especially, $TiO_2$ NP-induced impairment of cardiac hemodynamics and molecular mechanisms due to cardiac lesions are poorly understood.

Our previous studies indicated that exposure to $TiO_2$ NPs for 2, 3, or 6 consecutive months resulted in cardiac inflammation and atherosclerosis in mice; however, the interaction between cardiac hemodynamics and lesion mechanism were not evaluated.[22,23,25,26] The present study is focused on the changes of cardiac hemodynamics and expression of the cardiac lesions following exposure to $TiO_2$ NPs. The findings suggested that exposure to $TiO_2$ NPs increased the level of $TiO_2$ NPs accumulation in the mouse heart (Table II). This led to severe cardiac toxicity, shown by reductions of ATP production in the heart (Fig. 3), alterations of inflammation-related molecule expression (Table IV; Fig. 4), together with decreased body weight, increased cardiac indices (Table II), inflammation, tissue necrosis, bleeding congestion of blood (Fig. 1), apoptosis (Fig. 2), and altered cardiac hemodynamics (Table III). Accordingly, impairment of cardiac hemodynamics caused by $TiO_2$ NPs could be triggered by cardiac inflammation. The main results are discussed below.

Exposure to $TiO_2$ NPs was suggested to decrease antioxidant capacity with reductions of antioxidative enzymatic activities (such as superoxide dismutase, catalase, ascorbic acid peroxidase, glutathione-*S*-transferase, and glutathione reductase), and depletion of antioxidants (such as reduced glutathione and ascorbic acid), to increase ROS production, and to promote peroxidation of lipids and proteins, and DNA damage (increased 8-OHdg level), thus resulting in degeneration and necrosis of myocardial cell, inflammation,[22,25] atherosclerosis,[23] and mitochondrial injury (Fig. 2) in the mouse heart. These lesions may affect myocardial contraction and diastolic function.[46]

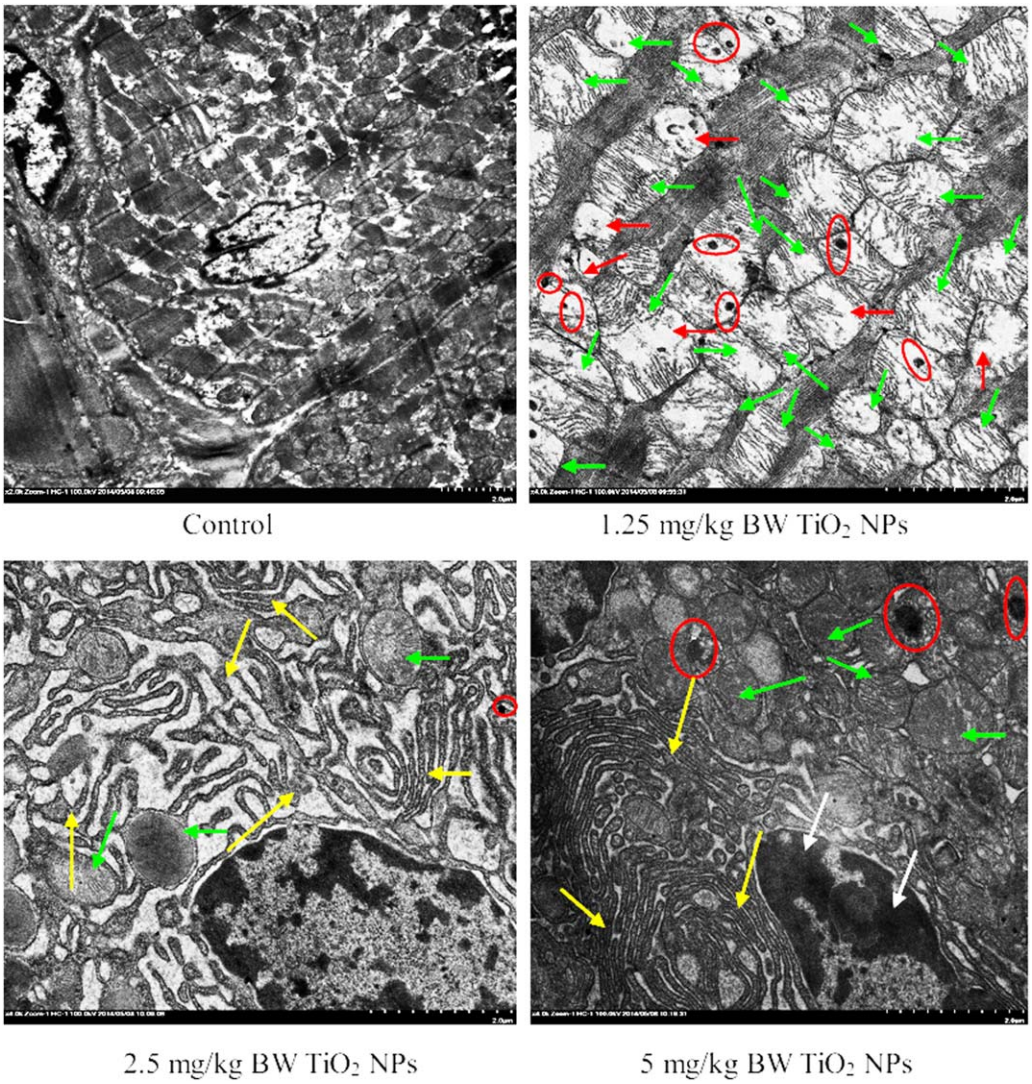


**FIGURE 2**. Ultrastructure observations of myocardial cells in mice following exposure to $TiO_2$ NPs for nine consecutive months (2000×). Green arrow indicates severe mitochondrial swelling, red arrow indicates disorder or disappearance of mitochondrial crest, red circle indicates $TiO_2$ NPs deposition; yellow arrow indicates endoplasmic reticulum dilation and swelling; white arrow indicates severe chromatin aggregation.

The contractile property of myocardium is the ability of the myocardium to produce contraction and relaxation after receiving effective stimulation. It is one of the important indexes of hemodynamics. As known, LVSP, LVEDP, DP, $dp/dt_{max}$, $dp/dt_{min}$, HR and CF are important indicators of cardiac function.[47–50] LVSP and $dp/dt_{max}$ are parameters of systole function. LVSP is elevated when preload or afterload is increased or the myocardial contractility is strengthened. To a certain extent, $dp/dt_{max}$ indicates the rate of the change of the increased tension of the ventricular wall, and is sensitive to the influence of various variable forces, but it is also involved in HR and preload or afterload. $dp/dt_{max}$ elevation or invariableness suggests enhancement of myocardial contractility when HR and preload or afterload are constant or reduced. Increased LVSP and $dp/dt_{max}$ display increased myocardial contractility.[47–50] Our data showed that $TiO_2$ NPs decreased LVSP and $dp/dt_{max}$, increased HR in the heart (Table III). $dp/dt_{min}$ is the sensitive indicator of early diastolic function of myocardial, represents the filling degree and diastolic function of the left ventricle as well as compliance, and easily influenced by LVSP afterload and HR. The change of LVEDP is related to the volume dilation and ventricular compliance of the ventricle, it can indirectly reflect the left ventricular diastolic function. LVEDP is increased when left ventricular diastole is insufficient or the amount of back effort is increased. In contrast, LVEDP is reduced when left ventricular systolic is strengthened or blood volume is decreased.[46–48] Heart rate (HR) indicates the rate of cardiac contraction. Coronary artery is the nutrition vessel of myocardium. Its diastolic effect directly affects CF. The abundant CF is essential for normal cardiac function. In the present study, $TiO_2$ NPs exposure increased LVEDP and HR, decreased $dp/dt_{min}$ and CF in the heart (Table III). The results mentioned above are main characteristics of systolic function of heart failure, and may be associated with reduction of body weight and cardiac lesions.

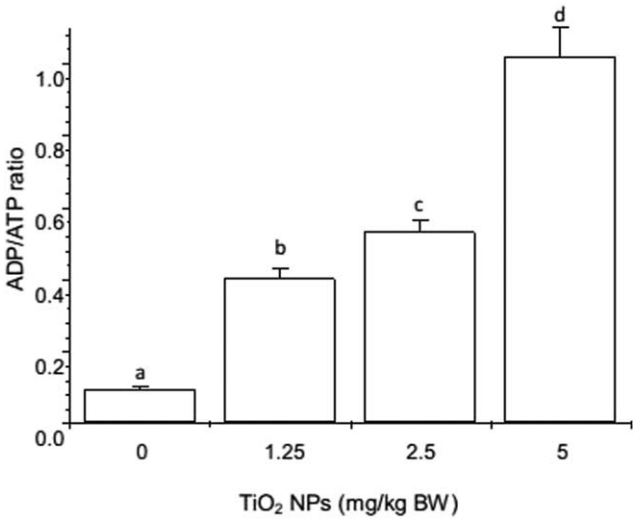


**FIGURE 3**. ATP production in the hearts of mice following exposure to $TiO_2$ NPs for nine consecutive months. Different letters in the same parameter indicate significant differences between groups ($p < 0.05$). Values represent mean ± SD ($N = 5$).

The sarcoplasmic reticulum (SR) is an intracellular membrane system in cardiac cells, which plays a dominant role in cardiac excitation–contraction coupling and cardiac contractility. A 1000-fold $Ca^{2+}$-gradient is maintained across the cardiac SR membrane by the SR $Ca^{2+}$-ATPase. The cardiac SR $Ca^{2+}$-ATPase can regulate intracellular $Ca^{2+}$-handling and thus, plays a crucial role in initiating cardiac contraction and relaxation. Quick removal of $Ca^{2+}$ into the SR or alternatively the extracellular lumen is essential for cardiac relaxation.[51] Decreased expression of SR $Ca^{2+}$-ATPase was demonstrated to impair cardiac contraction and relaxation in mice.[52] Our previous study showed that $TiO_2$ NPs can inhibit $Ca^{2+}$-ATPase activity,[26] which may be related to alterations of hemodynamics in mice (Table III). $Na^+/K^+$-ATPase catalyzes the transport of two $K^+$ in and three $Na^+$ out at the expense of one molecule of ATP, which are used in the management of congestive heart failure. The excitation–contraction coupling (ECC) of the ventricular cardiomyocytes is greatly dependent on the transport of $Ca^{2+}$ and $Na^+$ into and out of the cytoplasm. The decline in intracellular $Ca^{2+}$ concentration ($[Ca^{2+}]i$) is a prerequisite for

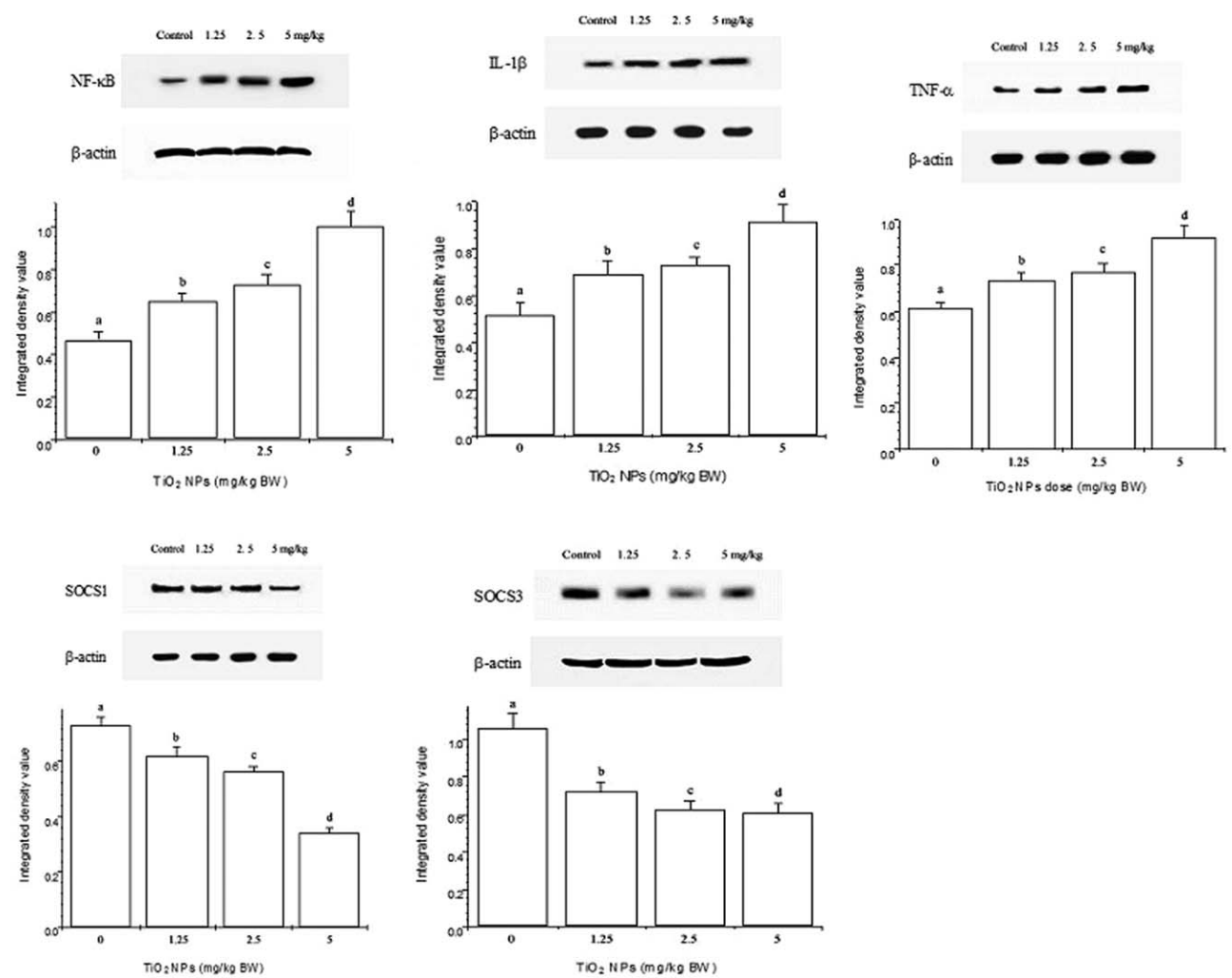


**FIGURE 4**. Effects of protein expression of inflammatory cytokines in the hearts of mice following exposure to $TiO_2$ NPs for nine consecutive months. Different letters in the same parameter indicate significant differences between groups ($p < 0.05$). Values represent mean ± SD ($N = 5$).

**TABLE IV. Effects of mRNA Expression of Inflammatory Cytokines in the Hearts of Mice Following Exposure to $TiO_2$ NPs for Nine Consecutive Months**

| | $TiO_2$ NPs (mg/kg BW) | | | |
|---|---|---|---|---|
| Gene/GAPDH | Control | 1.25 | 2.5 | 5 |
| NF-κB | 4.46 ± 0.26a | 5.46 ± 0.21b | 6.08 ± 0.45b | 7.22 ± 0.51c |
| IL-1β | 1.32 ± 0.12a | 1.94 ± 0.16b | 2.55 ± 0.13c | 2.76 ± 0.19c |
| TNF-α | 3.05 ± 0.21a | 4.91 ± 0.27b | 6.19 ± 0.41c | 6.22 ± 0.45c |
| SOCS1 | 26.15 ± 1.86a | 20.40 ± 1.91b | 18.59 ± 1.22b | 16.24 ± 1.35c |
| SOCS3 | 20.83 ± 1.58a | 16.09 ± 1.07b | 8.88 ± 0.55c | 6.99 ± 0.37c |

Different letters in the same parameter indicate significant differences between groups ($p < 0.05$). Values represent mean ± SD ($N = 5$).

cardiomyocyte relaxation. An important physiological role proposed for $Na^+/K^+$-ATPase is the regulation of blood pressure via modulation of vascular smooth muscle contractility.[53,54] With hypertension, heart failure, and diabetes, conditions known to have a vascular involvement, cardiac $Na^+/K^+$-ATPase expression has been reported to be changed.[55] Increasing smooth muscle $Na^+/K^+$-ATPase decreases blood pressure.[56] Evidence indicates that the $Na^+/K^+$-ATPase enzymatic activity is reduced in the failing human heart.[57] The activation of SR $Ca^{2+}/Mg^{2+}$ ecto-ATPase by various concentrations of $Ca^{2+}$ has been demonstrated to exhibit a linear relationship with an increase in cardiac muscle contractile force development. Based on the biochemical, electrophysiological and pharmacological evidence, it was proposed that the SR $Ca^{2+}/Mg^{2+}$ ecto-ATPase may serve as a biochemical correlate of the electrophysiologically defined $Ca^{2+}$ channels in heart sarcolemma. The SR $Ca^{2+}/Mg^{2+}$ ecto-ATPase participates in the degradation of extracellular ATP, which activates the SR $Ca^{2+}$ channel for $Ca^{2+}$-influx into cardiac myocytes.[58] Importantly, heart is highly dependent on continuous ATP delivery from mitochondrial substrate oxidation to main cardiac pump function. Impairment in mitochondrial function is observed in numerous cardiac pathologies, including the diabetic and the failing heart.[59,60] In our studies, $TiO_2$ NPs resulted in reductions of $Na^+/K^+$-ATPase, $Ca^{2+}/Mg^{2+}$-ATPase,[26] and ATP in the heart (Fig. 3), which may be associated cardiac mitochondrial damages **(**Fig. 2) and trigger cardiac contraction and relaxation(Table III). Our previous studies also suggested that $TiO_2$ NPs inhibited activities of $Ca^{2+}$ -ATPase, $Na^+/K^+$-ATPase, $Ca^{2+}/Mg^{2+}$-ATPase, and increased the contents of Ca, and Na, and decreased K content in mouse brain, leading to reduction of spatial cognitive function,[61] and decreased $Ca^{2+}$-ATPase, $Na^+/K^+$-ATPase, ATP synthesis in rats primary cultured neurons, thus causing higher levels of $[Ca^{2+}]I$, activation of $Na^+$ channels or $K^+$ currents, and suppression of dendritic development.[62] The decreased activities of $Ca^{2+}$-ATPase, and $Na^+/K^+$-ATPase caused by $TiO_2$ NPs may result in a failure to regulate the accumulation of intracellular $Ca^{2+}$, $Na^+$ and extracellular $K^+$, and consequently disturbed ionic homeostasis and the physiological functions of heart, thereby impairing cardiac hemodynamics. It needs further study in future.

The relationship between myocardial function and myocardial inflammation has been evaluated. For example, it had been demonstrated that the negative effects on myocardial function in sepsis were mediated through TNF-α and IL-1β,[63] local myocardial TNF-α, IL-1β, and NOS2 levels were increased after lipopolysaccharide treatment and contribute to the development of left ventricular (LV) dysfunction including increased HR response, depression of ejection phase indexes of contractile function, peak $dp/dt_{max}$, and peak developed LV systolic pressures.[30,64–67] Furthermore, pro- and anti-inflammatory mediators are suggested to express within the heart in response to mechanical pressure overload,[68] receptor activator of NF-κB ligand can be activated by transverse aortic constriction and thus induce cytokine expression of cardiomyocytes, thereby activating and attracting inflammatory cells.[69] Kong et al indicated that increased expression of the pro-inflammatory cytokines TNF-α, IL-1β, IL-6, TGF-β, and IFN-γ is consistently induced in cardiac inflammation.[70] Therefore, to the same extent as on cardiac hemodynamics the interest has been placed on examining influence of $TiO_2$ NPs on cardiac inflammatory process. Changes in NF-κB, IκB, proinflammatory cytokines including IL-lβ, IL-4, IL-6, TNF-α, TGF-β, and IFN-γ, and anti-inflammatory cytokine IL-2, have been already stated by our previous studies in the mouse liver, kidney, lung, spleen, brain, testis, and heart following exposure to $TiO_2$ NPs.[11,12,14,21,26,71–73] As expected, the present study observed that the expression of NF-κB, IL-lβ, and TNF-α was also increased by exposure to $TiO_2$ NPs (Table IV; Fig. 4), companying with infiltration of inflammatory cells in the mouse heart (Fig. 1). As known, cytokines exert profound effects on numerous cell types and cellular processes, so, cytokine signals are under stringent control; the failure regulation of the duration and intensity of cytokine signaling is the cause of a number of chronic inflammatory and autoimmune diseases. Suppressor of cytokine signaling (SOCS) proteins are induced by these cytokines and function as components of a negative feedback loop that regulate initiation, intensity, duration, and quality of cytokine responses.[74,75] Loss- and gain-of-function studies have demonstrated the important role of SOCS1 and SOCS3 proteins in regulating the course of inflammation in cardiovascular diseases.[76] SOCS1 is a crucial negative regulator of IL- lβ and TNF-α–mediated immune responses and expression of chemokines that mediate trafficking of inflammatory cells into the retina.[77–80] To further confirm whether $TiO_2$ NPs may be associated with cytokine-mediated signal pathway

in the inflamed heart, we also evaluated alterations of SOCS1 and SOCS3 expression, indicating marked reductions in both SOCS1 and SOCS3 expression (Table IV; Fig. 4). These results suggest that decreased expression both SOCS1 and SOCS3 resulted in increases of inflammatory cytokine expression in the mouse heat, which in turn resulted in exacerbation of cardiac inflammation and impairment of cardiac hemodynamics in mice.

In summary, exposure to $TiO_2$ NPs could result in cardiac inflammation apoptosis, companying with increase of LVEDP, and HR, reductions of LVSP, $dp/dt_{max}$, $dp/dt_{min}$, and CF. Furthermore, these lesions are demonstrated to involve in lowered ATP production, and significant induction of proinflammatory cytokine expression. The finding exhibits new insight into the mechanisms of the $TiO_2$ NP-induced cardiovascular damage. Therefore, a better understanding of the effects that these and others nanoparticles have on human health is imperative before daily life, medical, and other uses.

## ACKNOWLEDGMENTS

This work was supported by the National Natural Science Foundation of China (grant No. 81473007, 81273036, 30901218), the National Natural Science Foundation of Jiangsu Province (grant No. BK20161306), the Top-notch Academic Programs Project of Jiangsu Higher Education Institutions (PPZY2015A018), and the Bringing New Ideas Foundation of Huaiyin Normal University (201510323053X).

## REFERENCES

1. Chen T, Yan J, Li Y. Genotoxicity of titanium dioxide nanoparticles. J Food Drug Anal 2014;22:95–104.
2. Kinsinger N, Tantuccio A, Sun M, Yan Y, Kisailus D. Photocatalytic titanium dioxide composite. J Nanosci Nanotechnol 2011;11: 7015–7021.
3. Zhang L, Gu FX, Chan JM, Wang AZ, Langer RS, Farokhzad OC. Nanoparticles in medicine: Therapeutic applications and developments. Clin Pharmacol Ther 2008;83:761–769.
4. Youns M, Hoheisel JD, Efferth T. Therapeutic and diagnostic applications of nanoparticles. Curr Drug Targets 2011;12:357–365.
5. Yang F, Jin C, Subedi S, Lee CL, Wang Q, Jiang Y, Li J, Di Y, Fu D. Emerging inorganic nanomaterials for pancreatic cancer diagnosis and treatment. Cancer Treat Rev 2012;38:566–579.
6. Fisher J, Egerton T. Kirk–Othmer Encyclopedia of Chemical Technology. New York: John Wiley; 2001.
7. Sun D, Meng TT, Loong H, Hwa TJ. Removal of natural organic matter from water using a nanostructured photocatalyst coupled with filtering membrane. Water Sci Technol 2004;49:103–110.
8. Kaida T, Kobayashi K, Adachi M, Suzuki F. Optical characteristics of titanium oxide interference film and the film laminated with oxides and their applications for cosmetics. J Cosmet Sci 2004;55: 219–220.
9. Esterkin CR, Negro AC, Alfano OM, Cassano AE. Air pollution remediation in a fixed bed photocatalytic reactor coated with TiO2. AIChE J 2005;51:2298–2310.
10. Choi H, Stathatos E, Dionysiou DD. Sol–gel preparation of mesoporous photocatalytic $TiO_2$ films and $TiO_2/Al_2O_3$ composite membranes for environmental applications. Appl Catal B:Environ 2006; 63:60–67.
11. Hong J, Wang L, Zhao XY, Yu XH, Sheng L, Xu BQ, Liu D, Zhu YT, Long Y, Hong FS. Th2 factors may be involved in $TiO_2$ NP-induced hepatic inflammation. J Agric Food Chem 2014;62:6871–6878.
12. Gui SX, Li BY, Zhao XY, Sheng L, Hong J, Yu XH, Sang XZ, Sun QQ, Ze YG, Wang L, Hong FS. Renal injury and Nrf2 modulation in mouse kidney following exposure to titanium dioxide nanoparticles. J Agric Food Chem 2013;61:8959–8968.
13. Hong FS, Hong J, Wang L, Zhou YJ, Liu D, Xu BQ, Yu XH, Sheng L. Chronic exposure to nanoparticulate $TiO_2$ causes renal fibrosis involving activation of the Wnt pathway in mouse kidney. J Agric Food Chem 2015;63:1639–1647.
14. Sang XZ, Li B, Ze YG, Hong J, Ze X, Gui SX, Sun QQ, Liu HT, Zhao XY, Sheng L, Liu D, Yu XH, Wang L, Hong FS. Toxicological mechanisms of nanosized titanium dioxide-induced spleen injury in mice after repeated peroral application. J Agric Food Chem 2013;61:5590–5599.
15. Iavicoli I, Leso V, Bergamaschi A. Toxicological effects of titanium dioxide nanoparticles: A review of *in vivo* studies. J Nanomater 2012;2012:964381.
16. Chang X, Zhang Y, Tang M, Wang B. Health effects of exposure to nanoTiO2: A meta-analysis of experimental studies. Nanoscale Res Lett 2013;8:51.
17. Shi H, Magaye R, Castranova V, Zhao J. Titanium dioxide nanoparticles: A review of current toxicological data. Part Fibre Toxicol 2013;10:15.
18. Czajka M, Sawicki K, Sikorska K, Popek S, Kruszewski M, Kapka-Skrzypczak L. Toxicity of titanium dioxide nanoparticles in central nervous system. Toxicol in Vitro 2015;29:1042–1052.
19. Gao GD, Ze YG, Li B, Zhao XY, Liu XR, Sheng L, Hu RP, Gui SX, Sang XZ, Sun QQ, Cheng J, Cheng Z, Wang L, Tang M, Hong FS. The ovarian dysfunction and its gene-expressed characteristics of female mice caused by long-term exposure to titanium dioxide nanoparticles. J Hazard Mater 2012;243:19–27.
20. Gao GD, Ze YG, Zhao XY, Sang XZ, Zheng L, Ze X, Gui SX, Sheng L, Sun QQ, Hong J, Yu XH, Wang L, Hong FS, Zhang XG. Titanium dioxide nanoparticle-induced testicular damage, spermatogenesis suppression, and gene expression alterations in male mice. J Hazard Mater 2013;258:133–143.
21. Hong FS, Wang YJ, Zhou YJ, Zhang Q, Ge YS, Chen M, Hong J, Wang L. Exposure to $TiO_2$ nanoparticles induces immunological dysfunction in mouse testis. J Agric Food Chem 2016;64:346–355.
22. Sheng L, Wang XC, Sang XZ, Ze YG, Zhao XY, Liu D, Gui SX, Sun QQ, Cheng J, Cheng Z, Hu RP, Wang L, Hong FS. Cardiac oxidative damage in mice following exposure to nanoparticlate titanium dioxide. J Biomed Mater Res A 2013;101A:3238–3246.
23. Yu XH, Zhao XY, Ze YG, Wang L, Liu D, Hong J, Xu BQ, Lin AA, Zhang C, Zhao Y, Li BY, Hong FS. Changes of serum parameters of $TiO_2$ nanoparticle-induced atherosclerosis in mice. J Hazard Mater 2014;280:364–371.
24. Liu HT, Ma LL, Zhao JF, Liu J, Yan JY, Ruan J, Hong FS. Biochemical toxicity of mice caused by nano-anatase $TiO_2$ particles. Biol Trace Elem Res 2009;129:170–180.
25. Hong FS, Wang L, Yu XH, Zhou YJ, Hong J. Toxicological effect of $TiO_2$ nanoparticle-induced myocarditis in mice. Nanoscale Res Lett 2015;10:326.
26. Yu XH, Hong FS, Zhang YQ. Cardiac inflammation involving in PKCε or ERK1/2-activated NF-κB signalling pathway in mice following exposure to titanium dioxide nanoparticles. J Hazard Mater 2016;313:68–77.
27. Mikkelsen L, Sheykhzade M, Jensen KA, Saber AT, Jacobsen NR, Vogel U, Wallin H, Loft S, Møller P. Modest effect on plaque progression and vasodilatory function in atherosclerosis—Prone mice exposed to nanosized $TiO_2$. Part Fibre Toxicol 2011;8:32.
28. Han SG, Newsome B, Hennig B. Titanium dioxide nanoparticles increase inflammatory responses in vascular endothelial cells. Toxicology 2013;306:1–8.
29. Faddah LM, Baky NAA, Mohamed AM, Al-Rasheed NM. Protective effect of quercetin and/or l-arginine against nano-zinc oxide-induced cardiotoxicity in rats. J Nanoparticle Res 2013;15:1520–1533.
30. Knuefermann P, Nemoto S, Misra A, Nozaki N, Defreitas G, Goyert SM, Carabello BA, Mann DL, Vallejo JG. CD14-deficient mice are protected against lipopolysaccharide-induced cardiac inflammation and left ventricular dysfunction. Circulation 2002; 106:2608–2615.
31. Ohta K, Nakajima T, Cheah AY, Zaidi SH, Kaviani N, Dawood F, You XM, Liu P, Husain M, Rabinovitch M. Elafin-overexpressing mice have improved cardiac function after myocardial infarction. Am J Physiol Heart Circ Physiol 2004;287:H286–H292.

32. Westermann D, Lettau O, Sobirey M, Riad A, Bader M, Schultheiss HP, Tschöpe C. Doxorubicin cardiomyopathy-induced inflammation and apoptosis are attenuated by gene deletion of the kinin B1 receptor. Biol Chem 2008;389:713–718.
33. Rubaj A, Rucinski P, Kutarski A, Dabrowska-Kugacka A, Oleszczak K, Zimon B, Trojnar M, Zapolski T, Drozd J, Tarkowski A, Wysokinski A. Cardiac hemodynamics and proinflammatory cytokines during biatrial and right atrial appendage pacing in patients with interatrial block. J Interv Card Electrophysiol 2013;37:147–154.
34. Brook RD, Rajagopalan S, III Pope CA, Brook JR, Bhatnagar A, Diez-Roux AV, Holguin F, Hong Y, Luepker RV, Mittleman MA, Peters A, Siscovick D, Jr Smith SC, Whitsel L, Kaufman JD. Particulate matter air pollution and cardiovascular disease: An update to the scientific statement from the American Heart Association. Circulation 2010;121:2331–2378.
35. Mills NL, Tornqvist H, Robinson SD, Gonzalez M, Darnley K, MacNee W, Boon NA, Donaldson K, Blomberg A, Sandstrom T, Newby DE. Diesel exhaust inhalation causes vascular dysfunction and impaired endogenous fibrinolysis. Circulation 2005;112:3930–3936.
36. Seaton A, Tran L, Aitken R, Donaldson K. Nanoparticles, human health hazard and regulation. J R Soc Interface 2010;7:S119–S129.
37. Kreyling WG, Semmler M, Erbe F, Mayer P, Takenaka S, Schulz H, Oberdörster G, Ziesenis A. Translocation of ultrafine insoluble iridium particles from lung epithelium to extrapulmonary organs is size dependent but very low. J Toxicol Environ Health A 2002; 65:1513–1530.
38. Warheit DB, Webb TR, Reed KL, Frerichs S, Sayes CM. Pulmonary toxicity study in rats with three forms of ultrafine-$TiO_2$ particles: Differential responses related to surface properties. Toxicity 2007; 230:90–104.
39. Yang P, Lu C, Hua N, Du Y. Titanium dioxide nanoparticles co-doped with $Fe^{3+}$ and $Eu^{3+}$ ions for photocatalysis. Mater Lett 2002;57:794–801.
40. Hu RP, Zheng L, Zhang T, Cui YL, Gao GD, Cheng Z, Chen J, Tang M, Hong FS. Molecular mechanism of hippocampal apoptosis of mice following exposure to titanium dioxide nanoparticles. J Hazard Mater 2011;191:32–40.
41. National Institute for Occupational Safety and Health. Outlines Guidance on Handling Titanium Dioxide ($TiO_2$). Atlanta: National Institute for Occupational Safety and Health; 2011.
42. Baan R, Straif K, Grosse Y, Secretan B, El Ghissassi F, Cogliano V. Carcinogenicity of carbon black, titanium dioxide, and talc. Lancet Oncol 2006;7:295–296.
43. Gallez F, Fadel M, Scruel O, Cantraine F, Courtois P. Salivary biomass assessed by bioluminescence ATP assay related to (bacterial and somatic) cell counts. Cell Biochem Funct 2000;18:103–108.
44. Pfaffl MW, Horgan GW, Dempfle L. Relative expression software tool (REST) for group-wise comparison and statistical analysis of relative expression results in real-time PCR. Nucleic Acids Res 2002;30:E36.
45. Andersen CL, Jensen JL, Ørntoft TF. Normalization of real-time quantitative reverse transcription-PCR data: A model-based variance estimation approach to identify genes suited for normalization, applied to bladder and colon cancer data sets. Cancer Res 2004;64:5245–5250.
46. Reeve JL, Szegezdi E, Logue SE, Ní Chonghaile T, O'Brien T, Ritter T, Samali A. Distinct mechanisms of cardiomyocyte apoptosis induced by doxorubicin and hypoxia converge on mitochondria and inhibited by Bcl-xl. J Cell Mol Med 2007;113:509–520.
47. Wada K, Fujimori A, Matsukawa U, Arai Y, Sudoh K, Yatsu T, Sasamata M, Miyata K. Intravenous administration of conivaptan hydrochloride improves cardiac hemodynamics in rats with myocardial infarction-induced congestive heart failure. Eur J Pharmacol 2005;507:145–151.
48. Hole LD, Larsen TH, Fossan KO, Limé F, Schjøtt J. Diazoxide protects against doxorubicin-induced cardiotoxicity in the rat. BMC Pharmacol Toxicol 2014;15:28.
49. Hardt SE, Geng YJ, Montagne O, Asai K, Hong C, Yang GP, Bishop SP, Kim SJ, Vatner DE, Seidman CE, Seidman JG, Homcy CJ, Vatner SF. Accelerated cardiomyopathy in mice with overexpression of cardiac Gsand a missense mutation in the $\alpha$-myosinmeavy chain. Circulation 2002;105:614–620.
50. Peña JR, Wolska BM. Differential effects of isoflurane and ketamine/inactin anesthesia on cAMP and cardiac function in FVB/N mice during basal state and -adrenergic stimulation. Basic Res Cardiol 2005;100:147–153.
51. Frank KF, Bolck B, Erdmann E, Schwinger RHG. Sarcoplasmic reticulum $Ca^{2+}$-ATPase modulates cardiac contraction and relaxation. Cardiovasc Res 2003;57:20–27.
52. Müller FU, Lewin G, Matus M, Neumann J, Riemann B, Wistuba J, Schütz G, Schmitz W. Impaired cardiac contraction and relaxation and decreased expression of sarcoplasmic $Ca^{2+}$-ATPase in mice lacking the CREM gene. Faseb J 2002. 10.1096/fj.02-0486fje.
53. Blaustein MP, Zhang J, Chen L, Hamilton BP. How does salt retention raise blood pressure? Am J Physiol Regul Integr Comp Physiol 2006;290:R514–R523.
54. Sweeney G, Klip A. Regulation of the $Na^+/K^+$-ATPase by insulin: Why and how? Mol Cell Biochem 1998;182:121–133.
55. McDonough AA, Velotta JB, Schwinger RH, Philipson KD, Farley RA. The cardiac sodium pump: Structure and function. Basic Res Cardiol 2002;97:I19–I24.
56. Pritchard TJ, Parvatiyar M, Bullard DP, Lynch RM, Lorenz JN, Paul RJ. Transgenic mice expressing $Na^+$-$K^+$-ATPase in smooth muscle decreases blood pressure. Am J Physiol Heart Circ Physiol 2007;293:H1172–H1182.
57. Barwe SP, Jordan MC, Skay A, Inge L, Rajasekaran SA, Wolle D, Johnson CL, Neco P, Fang K, Rozengurt N, Goldhaber JI, Roos KP, Rajasekaran AK. Dysfunction of ouabain-induced cardiac contractility in mice with heart-specific ablation of Na, K-ATPase $\beta$1-subunit. J Mol Cell Cardiol 2009;47:552–556.
58. Kannan S, Elimban V, Dakshinamurti K, Dhalla NS. Biophysical characterization of rat cardiac $Ca^{2+}/Mg^{2+}$ecto-ATPase(Myoglein). Mol Cell Biochem 1998;183:153–157.
59. Boudina S, Sena S, O'Neill BT, Tathireddy P, Young ME, Abel ED. Reduced mitochondrial oxidative capacity and increased mitochondrial uncoupling impair myocardial energetics in obesity. Circulation 2005;112:2686–2695.
60. Bugger H, Abel ED. Mitochondria in the diabetic heart. Cardiovasc Res 2010;88:229–240.
61. Hu RP, Gong XL, Duan YM, Li N, Che Y, Cui YL, Zhou M, Liu C, Wang H, Hong FS. Neurotoxicological effects and the impairment of spatial recognition memory in mice caused by exposure to $TiO_2$ nanoparticles. Biomaterials 2010;31:8043–8050.
62. Hong FS, Sheng L, Ze YG, Hong J, Zhou YJ, Wang L, Yu XH, Liu D, Xu BQ, Ze X. Suppression of neurite outgrowth of primary cultured hippocampal neurons is involved in impairment of glutamate metabolism and NMDA receptor function caused by nanoparticulate $TiO_2$. Biomaterials 2015;53:76–85.
63. Duncan DJ, Hopkins PM, Harrison SM. Negative inotropic effects of tumour necrosis factor-$\alpha$ and interleukin-1$\beta$ are ameliorated by alfentanil in rat ventricular myocytes. Br J Pharmacol 2007;150: 720–726.
64. Giroir BP, Johnson JH, Brown T, Allen GL, Beutler B. The tissue distribution of tumor necrosis factor biosynthesis during endotoxemia. J Clin Invest 1992;90:693–698.
65. Kapadia S, Lee JAG, Birdsall HH, Ma TS, Mann DL. Tumor necrosis factor gene and protein expression in adult feline myocardium after endotoxin administration. J Clin Invest 1995;96:1042–1052.
66. Baumgarten G, Knuefermann P, Nozaki N, Sivasubramanian N, Mann DL, Vallejo JG. *In vivo* expression of proinflammatory mediators in the adult heart after endotoxin administration: The role of toll-like receptor-4. J Infect Dis 2001;183:1617–1624.
67. Nemoto S, Vallejo JG, Knuefermann P, Misra A, Defreitas G, Carabello BA, Mann DL. *Escherichia coli* LPS induced LV dysfunction: Role of toll-like receptor-4 in the adult heart. Am J Physiol Heart Circ Physiol 2002;282:H2316–H2323.
68. Honsho S, Nishikawa S, Amano K, Zen K, Adachi Y, Kishita E, Matsui A, Katsume A, Yamaguchi S, Nishikawa K, Isoda K, Riches DW, Matoba S, Okigaki M, Matsubara H. Pressure-mediated hypertrophy and mechanical stretch induces IL-1$\beta$ release and subsequent IGF-1 generation to maintain compensative hypertrophy by affecting Akt and JNK pathways. Circ Res 2009;105:1149–1158.
69. Ock S, Ahn J, Lee SH, Park H, Son JW, Oh JG, Yang DK, Lee WS, Kim HS, Rho J, Oh GT, Abel ED, Park WJ, Min JK, Kim J.

Receptor activator of nuclear factor-kB ligand is a novel inducer of myocardial inflammation. Cardiovasc Res 2012;94:105–114.
70. Kong P, Christia P, Frangogiannis NG. The pathogenesis of cardiac fibrosis. Cell Mol Life Sci 2014;71:549–574.
71. Ma LL, Zhao JF, Wang J, Liu J, Duan YM, Liu HT, Li N, Yan JY, Ruan J, Wang H, Hong FS. The acute liver injury in mice caused by nano-anatase $TiO_2$. Nanoscale Res Lett 2009;4:1275–1285.
72. Cui YL, Liu HT, Zhou M, Duan YM, Li N, Gong XL, Hu RP, Hong MM, Hong FS. Signaling pathway of inflammatory responses in the mouse liver caused by $TiO_2$ nanoparticles. J Biomed Mater Res A 2011;96A:221–229.
73. Sun QQ, Tan DL, Ze YG, Sang XZ, Liu XR, Gui SX, Cheng Z, Cheng J, Hu RP, Gao GD, Liu G, Zhu M, Zhao XY, Sheng L, Wang L, Tang M, Hong FS. Pulmotoxicological effects caused by long-term titanium dioxide nanoparticles exposure in mice. J Hazard Mater 2012;235 – 236:47–53.
74. Naka T, Fujimoto M, Kishimoto T. Negative regulation of cytokine signaling: STAT-induced STAT inhibitor. Trends Biochem Sci 1999;24:394–398.
75. Hilton DJ, Richardson RT, Alexander WS, Viney EM, Willson TA, Sprigg NS, Starr R, Nicholson SE, Metcalf D, Nicola NA. Twenty proteins containing a C-terminal SOCS box form five structural classes. Proc Natl Acad Sci USA 1998;95:114–119.
76. Tamiya T, Kashiwagi I, Takahashi R, Yasukawa H, Yoshimura A. Suppressors of cytokine signaling (SOCS) proteins and JAK/STAT pathways: Regulation of T-cell inflammation by SOCS1 and SOCS3. Arterioscler Thromb Vasc Biol 2011;31:980–985.
77. Kimura A, Naka T, Nagata S, Kawase I, Kishimoto T. SOCS-1 suppresses TNF-alpha-induced apoptosis through the regulation of Jak activation. Int Immunol 2004;16:991–999.
78. Morita Y, Naka T, Kawazoe Y, Grusby MJ. Signals transducers and activators of transcription (STAT)-induced STAT inhibitor-1 (SSI-1)/suppressor of cytokine signaling-1 (SOCS-1) suppresses tumor necrosis factor alpha-induced cell death in fibroblasts. Proc Natl Acad Sci USA 2000;97:5405–5410.
79. Naka T, Narazaki M, Hirata M, Matsumoto T, Minamoto S, Aono A, Nishimoto N, Kajita T, Taga T, Yoshizaki K, Akira S, Kishimoto T. Structure and function of a new STAT-induced STAT inhibitor. Nature 1997;387:924–929.
80. Starr R, Willson TA, Viney EM, Rayner JR, Jenkins BJ, Gonda TJ, Alexander WS, Metcalf D, Nicola NA, Hilton DJ. A family of cytokine-inducible inhibitors of signalling. Nature 1997;387:917–921.